# Bufalin Induced Mitochondrial Dysfunction Promotes Apoptosis of Glioma Cells by Regulating Annexin A2 and DRP1 Proteins

**Yao Li**
Northwest University
**Yan Zhang**
Xi'an Hospital of Traditional Chinese Medicine
**Xufang Wang**
Northwest University
**Qian Yang**
Air Force Medical University
**Xuanxuan Zhou**
Air Force Medical University
**Junsheng Wu**
Northwest University
**Xu Yang**
Northwest University
**Yani Zhao**
Xi'an Hospital of Traditional Chinese Medicine
**Rui Lin**
Air Force Medical University Xijing Hospital: Xijing Hospital
**Yanhua Xie**
Northwest University
**Jiani Yuan**
Air Force Hospital of Western Theater Command
**Xiaohui Zheng**
Northwest University
**siwang Wang** ( wangsiw@fmmu.edu.cn )
Northwest University https://orcid.org/0000-0003-1888-4716

**Primary research**

**Keywords:** Bufalin, glioma cell, mitochondrial dysfunction, DARTS-PAGE technology, Annexin A2, DRP1

**Posted Date:** May 5th, 2021

**DOI:** https://doi.org/10.21203/rs.3.rs-457826/v1



**Version of Record:** A version of this preprint was published at Cancer Cell International on August 10th, 2021. See the published version at https://doi.org/10.1186/s12935-021-02137-x.

# Abstract

**Background:** Glioma is a common primary central nervous system tumor, and there is still a lack of effective therapeutic drugs that can effectively improve the survival rate of patients in clinical. Bufalin has a good effect in the treatment of various tumors, but the mechanism of how it promotes the apoptosis of glioma cells is still unclear. The aim of this study was to investigate the drug target of bufalin acting on glioma cells, and to clarify the mechanism of apoptosis.

**Methods:** Cell viability and proliferation were evaluated by cck-8 and colony formation assay. Then, the cell cycle and apoptosis, intracellular ion homeostasis, oxidative stress levels and mitochondrial damage were detected after bufalin treatment. DARTS-PAGE technology combined with LC-MS/MS were employed to explore the drug targets of bufalin on U251 cells. Molecular docking and western blot were used to further identify the potential targets. siRNA of Annexin A2 and a DRP1 protein inhibitor Mdivi-1 were also used to verify the target of bufalin.

**Results:** Bufalin upregulated the expression of cytochrome C, cleaved caspase 3, p-Chk1 and p-p53 proteins to cause U251 cell apoptosis and cycle arrest in S phase. Bufalin can also induce oxidative stress in U251 cells, destroy intracellular ion homeostasis, and cause mitochondrial damage. The expression of mitochondrial separation/fusion-related proteins in U251 cells was abnormal, Annexin A2 and DRP1 protein were translocated from cytoplasm to mitochondria, and MFN2 protein was released from mitochondria into cytoplasm after bufalin treatment, which disrupted the mitochondrial division/fusion balance of U251 cells.

**Conclusions:** Our research indicated that bufalin can cause Annexin A2 and DRP1 oligomerization to be located on the surface of mitochondria, and disrupt the mitochondrial division/fusion balance to induce U251 cell apoptosis.


# Introduction

Glioma is the most common intracranial primary malignant tumor of the central nervous system, accounting for about 50–60% of intracranial primary tumors, and highly malignant of glioblastoma accounting for approximately 45% in all type of glioma [1, 2]. Because of its invasive growth, it can invade the surrounding normal brain tissue. After traditional surgical resection, the recurrence rate is very high. Therefore, besides operation, a combination of radiotherapy and chemotherapy to damage and destroy the DNA of glioma cells was applied as standard clinical treatment method. Temozolomide is an alkylating anti-tumor drug with high oral bioavailability and easy penetration through the blood-brain barrier [3]. It is currently the first-line drug for clinical treatment of glioma. After temozolomide enters tumor cells, its decomposition products can cause DNA methylation, which can interfere with cell DNA replication, cause DNA damage, and achieve anti-tumor effects [4]. However, the use of temozolomide in the treatment of gliomas is prone to drug resistance, and the clinical effective rate of glioma patients

using temozolomide is less than 45% [5]. Hence, it is important to exploit a new drug that can target the treatment of glioma effectively.

The drug affinity responsive target stability (DARTS) technology was first proposed and studied by Lomenick in 2009 [6]. Researchers found that specific DNA binding sites combined with their corresponding transcription factors have anti-Dnase degradation properties. Therefore, it is hypothesized that the target protein may be resistant to protease hydrolysis after binding with drugs. It is found that the complex obtained by co-incubation of FKBP12-rapamycin and FK506 could not be destroyed by subtilisin, which verifies the feasibility of the DARTS experiment. Hence, DARTS began to be used in drug target identification research [7].

Bufalin (Fig. S1) is the main active ingredient of Chan Su, which is extracted from the venom of *Bufo gargarizans Cantor* or *B.melan ostictus Schneider*. Its chemical name is 3β,14 -Dihydroxy-5β,20(22)-bufadienolide, and the content in dry toad venom can be as high as 1%～5% [8]. Numerous studies have shown that bufalin has an excellent inhibitory effect on prostate cancer cells, cervical cancer cells, leukemia cells, non-small cell lung cancer cells and glioma cells [9–12]. Bufalin had been reported that it had a digoxin-like effects, which manifested as the inhibition of the activity of $Na^+/K^+$-ATPase [13]. Some researchers found that bufalin can bind to $Na^+/K^+$-ATPase, inhibit sodium potassium pump, and further increase the intracellular calcium ion concentration, cause internal plasma reticulum stress eventually trigger cell apoptosis [14]. Bufalin can inhibit the proliferation, colony formation and stem cell-like phenotype of U87 and U251 cells by increasing the expression of miR-203 [15]. Bufalin can also up-regulate the expression of apoptotic protein such as cleaved caspase 3 and poly ADP ribose polymerase, down-regulate the expression of telomerase reverse transcriptase, induce apoptosis of glioma-like stem cells, and increase the sensitivity of glioma cells to temozolomide [16]. However, the mechanism of bufalin-induced oxidative stress mediated mitochondrial dysfunction in cell apoptosis is still unclear. Therefore, we use DARTS-PAGE technology combined with silver staining, LC-MS/MS and molecular biology techniques to further study the molecular mechanism of bufalin anti-glioma effects and to provides experimental evidence for its clinical application.

# Materials And Methods

### Cell culture and reagents

U251 cell line was purchased from Shanghai Cell Bank (Shanghai, China) and cultured in high-glucose DMEM (Thermo Fisher, USA) supplemented with 10% fetal bovine serum (FBS) and 1% antibiotics (100 U/mL penicillin G and 0.1 mg/mL streptomycin), then maintained in the exponential growth phase in an atmosphere of 5% $CO_2$ at 37°C. Bufalin (≥ 98% in purity) was purchased from BaoJi Chenguang Technology Development Co., Ltd. (Baoji, Shaanxi, China).

### Cell viability assay

The cell counting kit-8 (Dojindo Laboratories, Tokyo, Japan) was used to detect cell viability. U251 cell ($5\times10^3$ cells/well) was seeded in 96-well plates and cultured overnight, replace the culture medium with different concentrations of bufalin, and 10% FBS culture medium (0.1% DMSO) as the control well. After incubation for 12 h, 24 h, and 48 h, discard the culture medium and added 100 μL CCK-8 working solution.

### Clone formation assay

The U251 cells treated with 25 nM, 50 nM, and 100 nM bufalin for 24 h were seeded on a new 6-well plates at a density of 100 cells/well, then incubated at 37°C in a 5% $CO_2$ for 1 week. After Giemsa staining (Solarbio Science & Technology, Beijing, China), the clone formation rate was calculated as follows: clone formation rate (%) = numbers of clones/numbers of inoculated cells×100%.

### Cellular ATP content detection

The ATP assay (Merck, Darmstadt, Germany) was used to detect cellular ATP content. Cells treated with different concentrations of bufalin were digested with trypsin and collected, centrifuged for 5 min at 1500 rpm. The 10 μL cell suspension with density of $10^4$ cells were transferred into the luminometer plate and add 100 μL nucleotide lysate. After 5 min, 10 μL ATP detection working solution was added to the cell lysate and measure the luminescence level of each well within 1 to 2 minutes with fluorescence microplate reader. Follow the steps in the instructions to draw a standard curve and calculate the ATP content of each well.

### $Na^+/K^+$-ATPase activity assay

Collect the cells treated with 25 nM, 50 nM, and 100 nM bufalin for 24 h, add 1 mL extract into each tube (adjusting cells at density of $1\times10^6$ cells/mL in each group), sonicate the cells at the condition of power 20%, ultrasound 3 s, interval 10 s, repeat 30 times. Then centrifuge for 10 min at 8000 g under 4°C. The supernatant was transferred to 2 mL centrifuge tubes, and the enzymatic reaction and phosphorus determination were carried out according to the instructions of the $Na^+/K^+$-ATPase activity kit (Solarbio Science & Technology, Beijing, China). 200 μL samples were taken into 96-well plate and measure the absorbance at 660 nm.

### Intracellular $Ca^{2+}$ level assay

Intracellular Calcium ions level was measured according to the manufacturer's instruction. The Fluo 3-AM storage solution (1 mM) was prepared by dissolving 50 mg Fluo 3-AM powder (Dojindo Laboratories, Japan) with 44.2 μL DMSO and stored at -20°C away from light. Further, the Fluo 3-AM working solution (5 μM) was prepared by dissolving 44.2 μL Fluo 3-AM storage solution and 16.2 μL Pluronic ® F-127 (20% solution in DMSO, Invitrogen ® , Thermo Fisher Scientific) with 8.80 mL Hanks' Balanced Salt Solution (Gibco ® HBSS, Thermo Fisher Scientific). Briefly, the cells were seeded in confocal dishes overnight, then exposed to bufalin at the concentrations of 25 nM, 50 nM, and 100 nM in the fresh culture

medium, respectively. After 24 h, the cells were washed by PBS three times and inoculated with 1.5 mL/dish Fluo 3-AM working solution for 45 min in the dark cell incubator and then washed with PBS. The cells were continuously incubated with HBSS at 37°C with 5% $CO_2$ for 20 min to ensure the complete de-esterification of Fluo 3-AM. The fluorescence intensities were measured at $\lambda_{ex}$ / $\lambda_{em}$ = 490/520 nm by Olympus FV1000 confocal microscope (Olympus; Center Valley, PA, USA).

### Reactive oxygen species (ROS) assay

The reactive oxygen species (ROS) detection storage solution was prepared by dissolving ROS detection reagent (1vl, Sigma-Alorich, St. Louis, MO, USA) with 40 μL DMSO and stored at 4°C in the dark. 5000 cells were inoculated in a confocal culture dish. After they adhered to the wall, the cells were exposed to 25, 50 and 100 nM bufalin for 24 h. 2 mL of ROS detection reagent working solution was added in each dish and incubate at 37°C for 40 min in the dark. Wash the cells with PBS solution 3 times, add 2 mL PBS solution to each dish to cover the cells, and the fluorescence intensities were measured at $\lambda_{ex}$ / $\lambda_{em}$ = 490/520 nm by Olympus FV1000 confocal microscope (Olympus; Center Valley, PA, USA).

### Glutathione (GSH) assay

The intracellular GSH level was measured by GSH/GSSG-Glo Assay kit (Solarbio Science & Technology, Beijing, China). U251 cells treated with different concentrations of bufalin for 24 h were collected, and the contents of GSH and GSSG in each group of cells were determined according to the instructions of the GSH and GSSG activity assay kit, and then the GSH/GSSG ratio was calculated.

### Flow cytometry (FCM)

The cells were collected in the aseptic tubes after drug treatment, added 490 μL assay buffer, 5.0 μL Annexin V labeled with fluorescein (FITC-Annexin V) and 5.0 μL Propyridine iodide (PI) to incubate for 20 min and detected by FCM. According to the staining results, the proportion of living cells (Annexin V-/PI-), early apoptotic cells (Annexin V+/PI-), late apoptotic cells and necrotic cells (Annexin V+/PI+) can be distinguished in each group.

Cell cycle analysis was carried out by FCM. Through the combination between PI and DNA, FCM could divide the cell stage directly from the response of fluorescence intensity to DNA content. G1/G0 phase cells have DNA content of diploid cells, G2/M phase cells have DNA content of tetraploid cells, and S phase cells have DNA content between diploid and tetraploid cells. After collecting the cells treated with drugs, fixed them with 70% ethanol and overnight at 4℃. After PBS washing, PI staining solution containing RNA enzyme was added in the tubes. The cells were incubated at 37°C for 30 min and subsequently detected by FCM.

### Cell apoptosis analysis

The Mitotracker red CMX Ros kit (Beyotime Biotechnology, Shanghai, China) was used to probe apoptosis of U251 cells treated with 25, 50 and 100 nM bufalin for 24 h. Use Olympus FV1000 confocal microscope

to detect red fluorescence at $\lambda_{ex}$ / $\lambda_{em}$ = 579/599 nm, green fluorescence at $\lambda_{ex}$ / $\lambda_{em}$ = 492/520 nm, and blue fluorescence at $\lambda_{ex}$ / $\lambda_{em}$ = 350/461 nm.

### Transmission electron microscopy (TEM)

The cells treated with different concentrations of bufalin for 24 h were digested and collected in a centrifuge tube. After washing twice with PBS, 2.5% glutaraldehyde solution was added along the tube wall to cover the cell clumps, and the cells were allowed to stand overnight at 4°C. Wash 2 times with PBS, fix with 1% osmium acid, gradient dehydration, embed, make ultrathin sections, and stained with 2% uranyl acetate for 5 min. Observe the ultrastructure changes of cells under TEM.

### Mitochondrial membrane potential (MMP) assay

MMP was determined using Mitochondria Membrane Potential Kit (Sigma-Alorich, St. Louis, MO, USA) containing JC-10 dye. U251 cells were added into confocal Petri dishes ($1\times10^5$cells/dish) and dealt with 25, 50 and 100 nM bufalin for 24 h. After this, the medium was discarded and washing with PBS, add 2 mL of JC-10 working solution to each dish to cover the cells, and incubate at 37°C in the dark for 40 minutes. Then washing with PBS, observe the fluorescence intensity under the confocal microscope and calculate the ratio of red/green fluorescence.

### Western blot

Proteins from cells treated with bufalin for 24 h or samples after bufalin incubation with U251 cell total protein were separated by SDS electrophoresis. The following primary antibodies were used: cytochrome C, caspase 3 and cleaved caspase 3 (Cell Signaling Technology, Danvers, MA, USA), DRP1, HSPA8, HSPA9, TUBB, Annexin A2, and mitochondrial fusion protein-2 (MFN2) (Wanleibio Technology, Shenyang, China), GAPDH (Sigma-Aldrich, St. Louis, MO, USA) and COX IV (Wanleibio Technology, Shenyang, China) were used as the internal control followed by a secondary antibody conjugated with horseradish peroxidase (HRP; Santa Cruz). Western blotting was performed for three times. The intensity of each band was quantified with Image J.

### Drug affinity responsive target stability (DARTS) assay

Total protein of U251 cells was extracted, add 66 μL of 10×TNC solution to 600 μL of total protein after BCA quantification, divide into three aliquots, add 2.0 μL of DMSO, 100 μM, and 1000 μM bufalin respectively, mix gently, and incubate overnight in a refrigerator at 4℃. Take 50 μL of the cell protein extract combined with the drug, add 2.0 μL of 1×TNC, 1.25 mg/mL, and 0.25 mg/mL pronase working solution respectively, enzymatically digest at room temperature for 15 min, add 5×loading buffer for denaturation. Separate proteins by SDS-PAGE electrophoresis, and perform LC-MS/MS analysis after silver staining in accordance with the protocol of pierce silver stain kit (Thermo Fisher, USA)

### LC-MS/MS and proteomics analysis

SCIEX's Triple TOF 5600 LC-MS/MS system was used to perform mass spectrometry analysis of the differential bands, the peptide sample bound to the C18 capture column was gradient eluted to the analytical column. Ultrapure water with 0.1% formic acid (A) and acetonitrile with 0.1% formic acid (B) constituted the mobile phase, and the gradient elution programs as follows: 0 min-15 min, 5%–35% B; 15 min-16 min, 35%–80% B; 16 min-21 min, 80% B; 21 min-21.1 min, 80%–5% B; 21.1 min-29 min, 5% B. The flow rate was 0.3 μL/min. Mass spectrometry IDA mode analysis includes one MS full scan (at m/z 350–1500, 250 ms) in each scan cycle, followed by 40 MS/MS scans (at m/z 100–1500, 50 ms). MS/MS Collect the precursor ion signal greater than 120 cps, the charge number is +2–+5, and the exclusion time of repeated ion collection was set to 18 s.

The mass spectrum data is retrieved by ProteinPilot (V4.5), the database retrieval algorithm is Paragon, and the human proteome reference database in UniProt was used. The search results are screened with Unused ≥ 1.3 as the standard, the entries and contaminating proteins searched in the anti-database are deleted, and the remaining identification information was analysis followed-up.

## Molecular docking

The MOE-DOCK module was used to dock and predict the affinity of the ligand and the receptor. Small molecule drugs are defined as ligands, and proteins are defined as receptors. The 3D structure of the protein Annexin A2, TUBb, DRP1, HSPA9 and HSPA8 were downloaded from RCSB Protein Data Bank (http://www.rcsb.org/). With LigX, the protonation state and hydrogen orientation of the protein are optimized under the conditions of pH 7 and temperature 300K. The docking process adopts a flexible induced fit mode, the side chain of the amino acid binding pocket can be optimized and adjusted according to the ligand conformation, and the weight of restraining side chain rotation was set to 10. Each ligand produces a total of 1000 conformations, all docked poses of which were ranked by London dG scoring first, and the top 30 poses were rescoring by GBVI/WSA dG method, respectively. Finally, the representative conformation was selected based on the binding score. The interaction mode of ligand and receptor is mapped by software PyMOL (www.pymol.org).

## Small interfering RNA transfection

The U251 cells was seeded in a 6-well plate at a density of $1\times10^6$ cells/well. Use lipofectamineTM 2000 reagent to transfect Annexin A2 siRNA (GenePharma, shanghai, China) with the sequence 5'-TGTGTGGTGGAGATGACTGA-3' into U251 cells for transfection with humans. The genomic sequence without any matching negative siRNA was used as the negative control group, and only U251 cells with lipofectamineTM 2000 reagent were used as the mock control group. After Annexin A2 siRNA was transfected into U251 cells for 72 h, Western blot was used to detect the expression level of Annexin A2 protein in cells.

## Statistical analysis

Each experiment was performed at least three times and analyzed by GraphPad Prism 7 software. The data are expressed as mean ± SD. *P* values were calculated using the one-way ANOVA when the variances are uniform, and if the variances are not uniform, nonparametric tests are used for statistical analysis. $P < 0.05$ was considered statistically significant.

## Results

# Bufalin induces U251 cell apoptosis and intracellular oxidative stress

To examine the effect of bufalin in U251 cells, we treated U251 cell line with different concentrations of bufalin for 12 h, 24 h and 48 h, and performed cck-8, colony formation and cell apoptosis detect. The results showed that bufalin has a significant proliferation inhibitory effect on U251 cells, which can lead to loss in cell viability and colony formation, increase the proportion of apoptotic cell populations (S Fig. 2A, B, and F). The Fluo 3-AM staining and $Na^+/K^+$-ATPase activity kit were employed to detect the activity of $Na^+/K^+$-ATPase and $Ca^{2+}$ content in U251 cells after bufalin treatment. The results showed that bufalin can inhibit the $Na^+/K^+$-ATPase activity and increase the $Ca^{2+}$ level in U251 cells in a dose-dependent manner (S Fig. 2C, D, and E).

We also observed the cell apoptosis induced by bufalin by co-staining with Mitotracker Red CMX Ros, Annexin V-FITC and Hoechst 33342, and further detect the apoptotic proteins by western blot. we found that the phosphatidylserine of U251 cells has everted from the inside of the plasma membrane to the cell surface and stained by Annexin V-FITC. It indicates that the U251 cells undergo early apoptosis after exposed to bufalin for 12 h (Fig. 1A). Electron microscopy revealed numerous vacuolar-like structures in bufalin treated cells, and the mitochondria, endoplasmic reticulum and other organelles were obviously damaged and scattered like fragments (Fig. 1B). The apoptosis related proteins result showed that bufalin can up-regulate the expression of cytochrome C protein and the active form of caspase 3 of cleaved caspase 3 ($p < 0.05$) to cause U251 cell apoptosis (S Fig. 2G).

The production of intracellular ROS and the consumption of GSH are two indicators of cellular oxidative stress. We detected the level of ROS and GSH and ATP content in U251 cells to observe the oxidative stress induced by bufalin. The results showed that the ROS level in U251 cells treated with bufalin was increased, with 4.93-fold increases in ROS level of 100 nM bufalin treated cells than that of control group (Fig. 1C and D), and the intracellular GSH/GSSG ratio and ATP content of bufalin-treated cells was significantly reduce, indicating that bufalin promotes GSH consumption and affected the ATP produce in U251 cells (Fig. 1E and F). Furthermore, it was found that NAC partially scavenged ROS increased by bufalin, and CCK-8 results also showed that pretreatment with 10 mM NAC for 1 h can partially inhibit the decrease in cell viability induced by bufalin (Fig. S3 A-C).

### Bufalin induces DNA damage and arrest the cell cycle at S phase

To assess whether the apoptosis of U251 cells caused by bufalin is related to cell cycle arrest. We performed flow cytometry to detect the U251 cell cycle after bufalin treatment. The results showed that bufalin treatment led to a concentration-dependent increase in cellular population in S phase indicating that bufalin-induced U251 cell apoptosis accompanied by an arrest at S phase (Fig. 2A).

The S-phase checkpoint detects whether the DNA is damaged and whether the damaged DNA molecule is repaired, so as to prevent the damaged DNA from being replicated and passed down. Therefore, we detected the mRNA levels of S-phase DNA damage molecule in U251 cells treated with bufalin by RT-QPCR, such as ATM, ATR, Chk1, Chk2, CDC25A and CDK2. The results indicate that the mRNA levels of Chk2 and ATM were significantly down-regulated, while the mRNA expression levels of Chk1, ATR, CDC25A and CDK2 were significantly up-regulated ($p < 0.05$ or $p < 0.01$) in U251 cells exposed to bufalin (Fig. 2C). At the same time, the protein levels of p-Chk1 and p-p53 in U251 cells treated with bufalin for 24 h were significantly up-regulated, and the expression levels of Chk1 and p53 proteins were significantly down-regulated, indicating that bufalin caused U251 cells to be blocked to S phase by regulating DNA damage-related genes (Fig. 2B).

# Bufalin Induces Mitochondrial Dysfunction In U251 Cells

JC-10 can be concentrated to form reversible red fluorescence in cells with polarized mitochondrial membrane. When the mitochondrial membrane potential decreases and JC-10 cannot accumulate in the matrix of mitochondria, JC-10 is a monomer and can produce green fluorescence. By calculating the ratio of red/green fluorescence, the MMP level in U251 cells can be determined to evaluate the effect of bufalin on cell mitochondrial function. Following 6 h of treatment with bufalin, the intracellular MMP level decreased in U251 cells (Fig. S4). 12 h and 24 h exposing to bufalin further reduced the level of MMP significantly (Fig. S4). Moreover, the level of MMP in the U251 cells treated with bufalin decreased with the increase of the administration concentration (Fig. 3A). These results indicating that bufalin can induce the loss of mitochondrial potential in a dose- and time- dependent manner.

Mitotracker Green staining was used to evaluate the mitochondrial morphology and function of U251 cells after bufalin treatment. The mitochondria in U251 cells without drug treatment are tightly distributed and the network is clear, while the mitochondrial of bufalin-treated cells are scattered and the network is relatively loose, and the mitochondrial fluorescence of the bufalin administration group was significantly lower than that of the control group (Fig. 3B).

TEM observation of the microscopic morphology of mitochondria of U251 cells found that bufalin can densify cell mitochondria and swell the cristae, increase the number density of mitochondria (Nv), and reduce the surface volume ratio (Rsv), volume density (Vv) and mitochondrial surface density (Sv) of mitochondria as shown in electron microscopic pictures (Fig. 3C-G). Based on these results, we suggest that bufalin can make U251 cells mitochondria split into more mitochondria with smaller size, thereby affecting mitochondrial function.

# Identification Of Bufalin Targets By Darts On U251 Cells

To clarify the target of bufalin acting on U251 cells, we silver-stained the SDS-PAGE gel that separated the total protein of U251 cells incubate overnight with bufalin, and numbered the bands with obvious differences as 0918-1, 0918-2...and 0918-7 according to the molecular weight (Fig. 4A). After decolorization, enzymolysis and extraction, it was detected and analyzed by TripeTOF 5600 LC-MS/MS. The mass deviation of all peptides is less than 20 parts per million, and the mass spectrometry detection accuracy is good, most peptides have no missing cleavage sites, and a small number of peptides have 1 or 2 missing cleavage sites, indicating that the digestion is sufficient and the sample preparation meets the standard (Fig. 4B). Based on the experience that the higher the protein abundance, the more spectra collected, the proteins with Unused ≥ 1.3 were screened out, and a total of 258 differential proteins were obtained. GO analysis of 258 differential proteins found that they are mainly involved in protein metabolism, energy channels, metabolism, cell growth/maintenance, protein folding, mitochondrial transport and immune response regulation and other key links in the proliferation of glioma cells (Fig. 4C).

### Target screening and verification of bufalin acting on U251 cells

The differential proteins including Annexin A2, TUBb, HSPA8, DRP1, HSPA9, PKM2, TKT, ENO1 and HSP90AB1 (Cloud-clone, Houston, America) were incubated with bufalin to verify their binding effect. The results showed that Annexin A2, DRP1, TUBb, HSPA8 and HSPA9 were not enzymatically digested after bufalin incubation, indicating that the potential direct target proteins of bufalin with U251 cells are Annexin A2, DRP1, TUBb, HSPA8 and HSPA9 (Fig. 5A).

The results of molecular docking showed that the oxygen atom of the hydroxyl group in bufalin acts as a hydrogen bond donor, bond with the oxygen atom of the side chain of Glu52 in Annexin A2, the main chain oxygen atom of Gly142 in TUBb, the side chain nitrogen atom of Glu313 in HSPA9, and the side chain oxygen atom of Asp218 in DRP1 forms a hydrogen bond (Fig. 5B, C, D, F). The oxygen atom of the hydroxyl group in bufalin also acts as a hydrogen bond acceptor, forming a hydrogen bond with the side chain oxygen atom of Tyr224 in TUBb, the side chain nitrogen atom of Ly316 in HSPA9, and the side chain oxygen atom of Lys56 in HSPA8 (Fig. 5C, D, E). The lactone oxygen atom in bufalin acts as a hydrogen bond acceptor, combined with the nitrogen atom of the side chain of Lys323 in Annexin A2, the side chain nitrogen atom of Lys121 in HSPA9, the side chain of Ser275 in HSPA8 and the main chain nitrogen atom of Ser39 in DRP1 to form hydrogen bonds (Fig. 5B, C, D, F). These results implicated that Annexin A2, DRP1, TUBb, HSPA8 and HSPA9 may be the targets of bufalin on U251 cells.

# Bufalin Binds Directly To Annexin A2 And Drp1 Protein

The total protein of U251 cells was incubated with bufalin and then enzymatically hydrolyzed and denatured. DARTS-Western blot experiment was used to further verify the direct binding ability of potential target protein with bufalin. The results showed that the direct binding ability of Annexin A2 and

DRP1 proteins was strong, and not easy to be hydrolyzed by protease after binding to bufalin (Fig. 6A), but HSPA9, TUBb and HSPA8 did not see the same trend (Fig. 6B). WB was used to detect whether bufalin treatment for 24 h affected the expression of HSPA8, HSPA9 and TUBb protein in U251 cells. The results showed that compared with the control group, the expression of HSPA9 protein increased significantly after the administration of 25 nM and 50 nM bufalin for 24 h ($p < 0.05$), while there was no significant change in the 100 nM bufalin group (Fig. 6C). There was no change of HSPA8 and TUBb protein expression in each administration group. Based on these results, we suggest that Annexin A2 and DRP1 proteins are the direct target proteins of bufalin acting on U251 cells.

### Bufalin regulated Annexin A2 and DRP1 proteins to disrupt the mitochondrial division/fusion balance

To verify the role of Annexin A2 and DRP1 in cell apoptosis promoted by bufalin, we examined the Annexin A2 protein in bufalin-treated U251 cells for 24 h. The results showed that 100 nM bufalin can significantly reduce the Annexin A2 protein content in U251 cytoplasm, while increase the Annexin A2 protein in mitochondria (Fig. 7A and B). We therefore investigated whether Annexin A2 is related to bufalin-induced apoptosis of U251 cells. A further decrease in cell viability treated with bufalin was by knockdown of Annexin A2 using siRNA (Fig. 7C and D).

The expression of mitochondrial division/fusion-related proteins DRP1 and MFN2 in U251 cells treated with different concentrations of bufalin were detected, and it was found that after bufalin treatment, the expression level of DRP1 protein in U251 cytoplasm was down-regulated and up-regulated in mitochondria (Fig. 7E and F). However, the expression of MFN2 protein was up-regulated in U251 cytoplasm, but down-regulated in mitochondria (Fig. 7E and F).

In addition, Mdivi-1 (DRP1 inhibitor) could attenuate the impact of bufalin on cell viability and mitochondrial structure changes. After pretreatment with 20 μM Mdivi-1, the cell viability of Mdivi-1 + bufalin group cells was increased compared with group without Mdivi-1 pretreatment (Fig. 7H). Mdivi-1 + bufalin can also slow down the decrease of ATP content in U251 cells caused by bufalin and protect its mitochondrial function (Fig. 7J). The effect of 20 μM Mdivi-1 pretreatment on the changes of mitochondrial structure induced by bufalin was observed by electron microscope. The Vv of the 50 nM bufalin group was significantly reduced, Rsv was significantly increased, and there was no significant difference between Nv and Sv, while the mitochondria of U251 cells in the Mdivi-1 group did not change, indicating that 50 nM bufalin can reduce the volume of mitochondria and change the structure of U251 cells (Fig. 7G and I). After pretreatment with 20μM Mdivi-1, compared with the control group, the Nv, Vv, Rsv, Sv of the Mdivi-1 + bufalin group did not change significantly, and compared with the 50 nM bufalin group, the Mdivi-1 + bufalin group Vv and Sv increased significantly, and there was no significant change in Nv and Rsv (Fig. 7G and I). In conclusion, these results indicated that bufalin can promote mitochondrial translocation of Annexin A2 and cause DRP1 oligomerization to be located on the surface of mitochondria, disrupt the mitochondrial division/fusion balance to induce U251 cell apoptosis.

# Discussion

Toad venom has a long history of treating tumors, and was recorded in "Compendium of Materia Medica" to "cure all malignant swelling". It is reported that bufalin as one of the main active ingredients of toad venom, has a killing effect on a variety of tumor cells, and combination of bufalin with 5-flurouracial can improve the drug resistance of tumor cells, reduce proliferation and induce apoptosis [17, 18]. The previous studies found that bufalin and its liposome could induce apoptosis of HepG2, HCT116, A549 and U251 cells *in vitro*, and inhibit the growth of nude mouse xenograft gliomas *in vivo* [19, 20]. In present study, the possible molecular mechanisms of bufalin how to inducing mitochondrial dysfunction to promote apoptosis in gliomas cells were elucidated.

This study has shown that bufalin can significantly inhibit the proliferation and colony formation of U251 cells, and cause structural loss of mitochondria and endoplasmic reticulum in the cells. The S-phase checkpoint is one of the important mechanisms of DNA damage repair, which detects whether the DNA of the cell is damaged and whether the damaged DNA molecule is repaired, so as to prevent the damaged DNA from being replicated and passed down [21–23]. The results of qRT-PCR experiments showed that the mRNA expression levels of Chk1, ATR, CDC25A and CDK2 in U251 cells treated with bufalin were significantly up-regulated, and the ATR-Chk1-CDC25A-CDK2 pathway was activated to transmit DNA damage signals, which directly caused U251 cell cycle arrest in S phase. The cytochrome C, caspase 3, c-myc, Chk1, p-Chk1, P53 and p-P53 protein expression levels in U251 cells were determined by western blot to verify the apoptosis and DNA damage proteins induced by bufalin. The results showed that bufalin can up-regulate cytochrome C expression, activate downstream caspase 3 protein phosphorylation, cause DNA damage, up-regulate c-myc, activate p53 signaling pathway, causing cell cycle arrest in S phase and inducing apoptosis.

The production of a small amounts of oxygen free radicals in cells can maintain the balance of oxygen metabolism under the action of free radical scavenging enzymes or antioxidants in the healthy conditions, but when excessive free radicals are generated by exogenous oxidants or the oxidation metabolism process, it exceeds the ability of anti-oxidant system and induce cell to a state of oxidative stress [24]. The decrease of GSH content is a potential early activation signal for apoptosis, and the subsequent production of oxygen free radicals promotes cells to enter apoptosis [25, 26]. We used DCFH-DA staining to determine the intracellular ROS content and the ratio of GSH/GSSG to evaluate the oxidative stress of U251 cells after bufalin treatment. The results show that bufalin can induce the overproduction of ROS in U251 cells, increase the consumption of GSH and the imbalance of redox in the cells. $Na^+/K^+$-ATPase is a protein embedded in the lipid bilayer of the plasma membrane of the cell, with enzymatic activity and carrier function [27, 28]. It can not only catalyze the hydrolysis of ATP to provide energy, but also drive the transport of $Na^+$ and $K^+$ on both sides of the cell membrane, maintain the membrane potential on both sides of the cell membrane, and play an extremely important role in maintaining the normal physiological functions of cells [29, 30]. However, due to the existence of $Na^+/Ca^{2+}$ exchange, the imbalance of sodium and potassium ions is likely to cause an imbalance of intracellular calcium ion homeostasis [31]. By detecting the activity of $Na^+$-$K^+$-ATPase and the level of $Ca^{2+}$ in U251 cells, it was found that bufalin can disrupt the homeostasis of $Na^+$, $K^+$ and $Ca^{2+}$ ions in U251 cells.

The imbalance of intracellular ions and the excessive generation of ROS will trigger the opening of the mitochondrial permeability transition pore, and the expression of cytochrome C protein will be up-regulated, which activates the downstream caspase 3 protein, causing tumor cell mitochondrial dysfunction, thereby inducing cell apoptosis [32]. Detection of cell mitochondrial membrane potential and intracellular ATP content were the important means to evaluate mitochondrial function [33]. MMP was measured by JC-10 staining, and cell ATP content was measured by ATP content determination kit. It was found that bufalin could induce a significant decrease in ATP content and MMP level in U251 cells, open mitochondrial permeability transition pore, and further induce mitochondrial dysfunction. Therefore, we believe that mitochondria play an important role in tumor cell apoptosis induced by bufalin.

DARTS is a new technology that based on the combination of small molecule drugs and their target proteins, which leads to a decrease in the sensitivity of target proteins to protease degradation. Since they do not require drug protective modification and have no drug activity dependence, they can be widely used in drug screening and target identification. The tool enzymes used in the DARTS technology that have been reported include subtilisin, thermolysin and pronase. Subtilisin is required to operate under alkaline conditions, which is more restrictive, and for small molecule drugs, the stability of non-target proteins is greatly improved after being combined with them [35]. However, pronase has strong activity under neutral pH conditions and can be specific cleavage of folded or unfolded proteins, as well as the carboxyl side peptide chains of glutamic acid and aspartic acid in polypeptide chains. Therefore, pronase was often used as tool enzymes in DARTS technology to identify targets for small molecule drugs [36]. DARTS-PAGE technology was employed to identify the target of bufalin to U251 cells. According to the results of silver staining, and perform LC-MS/MS analysis after enzymatic hydrolysis in the different gels. Based on the higher the protein abundance, the greater the number of spectra collected. The number of reference spectra is used to represent the abundance of the reactive protein in the sample, and a total of 258 differential proteins are obtained. On this basis, combined with protein molecular weight, peptides and number of spectra to determine the representative differential protein displayed on the SDS-PAGE gel. It was found that the potential direct target protein group included Annexin A2, TUBb, HSPA8, DRP1 HSPA9, PKM2, TKT, ENO1 and HSP90AB1. Western blot was used to detect the total protein of incubated with bufalin, and found that Annexin A2 and DRP1 are the direct target proteins of bufalin with U251 cells, while HSPA9, HSPA8 and TUBb proteins are less likely to be their direct target proteins.

Annexin A2 protein can enhance the activity of DNA polymerase and play an important role in DNA synthesis and cell proliferation [34, 35]. Its C-terminus can be combined with c-myc mRNA to regulate the function of c-myc gene. The protein encoded by c-myc gene can be used as a transcription factor to promote cell proliferation and play multiple physiological and pathological roles in tumor formation [36]. Studies have reported that Annexin A2 protein is a substrate of the EGFR/ras/MAPK/PKC signaling pathway [37]. When EGFR and Annexin A2 proteins are simultaneously highly expressed in human glioma cells, the role of the MAPK signaling pathway is significantly enhanced, thereby promote the aggressive growth of human glioma cells [38]. We found that after treated with 100 nM bufalin for 24 h, Annexin A2 protein expression in cytoplasm of U251 cells was significantly down-regulated, while Annexin A2 protein

expression in mitochondria was significantly up-regulated. Through siRNA technology, it was proved that after the expression level of Annexin A2 decreased, the cell survival rate of U251 cells was significantly reduced after bufalin treated, that is, the sensitivity of U251 cells to bufalin was enhanced. The above results indicating that bufalin treatment caused Annexin A2 protein to undergo mitochondrial translocation, and Annexin A2 silencing reduced the activity of U251 cells treated by bufalin and promoted cell apoptosis. Moreover, whether the autophagy caused by bufalin treatment is related to the regulation of Annexin A2, which causes cell apoptosis needs further study.

Mitochondrial division protein DRP1 is one of the key proteins that regulates mitochondrial division and fusion [39, 40]. The phosphorylation of DRP1 at Ser 616 can promote mitochondrial division, and when DRP1 is phosphorylated at Ser 637, mitochondrial division is inhibited [41]. Erk2, CaMKII, AMPK activation and Cdk1/cyclin B can promote the phosphorylation of DRP1 at Ser 616 and increase the translocation of DRP1 to the mitochondrial surface [42]. FIS1 can promote DRP1 to enter mitochondria from the cytoplasm, and then interact with DRP1 to promote mitochondrial fragmentation. Bax can migrate to the outer mitochondrial membrane to form a focal point, and then interact with DRP1 and MFN2 to regulate mitochondrial morphology and apoptosis [43, 44]. Under normal conditions, DRP1 protein is mainly distributed in the cytoplasm, and a small part is distributed in the mitochondria. When the mitochondria divide, DRP1 can wrap the mitochondrial outer membrane and split it into membrane-related tubular structures through oligomerization [45]. Through the GTP hydrolysis-dependent mechanism, these tubular structures wrap around the cutting point, shrinking and cutting the mitochondrial membrane [46]. In addition, DRP1 plays an important role in the process of mitochondrial mitosis and participates in the normal release of cytochrome C and the activation of caspase during apoptosis [47]. This study found that after bufalin treatment, the expression of mitochondrial division/fusion-related proteins in U251 cells was abnormal, DRP1 protein was translocated from cytoplasm to mitochondria, and MFN2 protein was released from mitochondria into cytoplasm, disrupting the mitochondrial division/fusion balance of U251 cells. The DRP1 protein inhibitor Mdivi-1 can partially ameliorate the abnormal structure of mitochondria in U251 cells caused by bufalin, protect mitochondrial function, and reduce the proportion of apoptotic cells. The above results all suggest that DRP1 protein is involved in the process of bufalin-induced mitochondrial structure and function abnormalities in U251 cells, which ultimately leads to cell apoptosis.

This study disclosed a novel mechanism of bufalin in cell apoptosis via regulation of Annexin A2 and DRP1 proteins to cause mitochondrial dysfunction in U251 cells, and to provide a foundation for the clinical application.

# Abbreviations

DARTS, drug affinity responsive target stability; FCM, flow cytometry; GSH, Glutathione; IC50, inhibitory concentration; MMP, Mitochondrial membrane potential; NAC, N-acetylcysteine; Nv, number density of mitochondria; ROS, reactive oxygen species; Rsv, surface volume ratio; Sv, surface density; TEM, transmission electron microscopy; Vv, volume density.

# Declarations


### Acknowledgements

Not applicable.


### Authors' contributions

YL and YZ designed and completed the experiment; XFW, QY, XXZ, and JSW assisted in the completion of some experiments; XY, YNZ, RL, and YHX analyzed the data and completed the figure; JNY wrote the original draft; XHZ and SWW checked the experimental design and implementation, revised the manuscript and provide research funding. All authors read and approved the final manuscript.


### Funding

This work was supported by Science and Technology Innovation Project of Shaanxi province in China (no.2015SF2-08-01), a grant from the Social Development of Shaanxi Province Key Project (no.2017ZDXM-SF-019, S2018-ZC-GCZXXY-SF-0005), and Shaanxi Key Laboratory of Biomedicine (no.2018SZS41).


### Availability of data and materials

The data and materials that support the current study are available from the corresponding author on reasonable request.

### Ethics approval and consent to participate

Not applicable.

### Consent for publication

Not applicable.

### Competing interests

The authors have no conflicts of interest to declare.

# References


1. Davis ME. Epidemiology and Overview of Gliomas. Seminars in oncology nursing 2018, 34(5):420–429.
2. Lah TT, Novak M, Breznik B. Brain malignancies: Glioblastoma and brain metastases. Sem Cancer Biol. 2020;60:262–73.

3. Karachi A, Dastmalchi F, Mitchell DA, Rahman M. Temozolomide for immunomodulation in the treatment of glioblastoma. Neurooncology. 2018;20(12):1566–72.
4. Choi S, Yu Y, Grimmer MR, Wahl M, Chang SM, Costello JF. Temozolomide-associated hypermutation in gliomas. Neurooncology. 2018;20(10):1300–9.
5. Jiapaer S, Furuta T, Tanaka S, Kitabayashi T, Nakada M. Potential Strategies Overcoming the Temozolomide Resistance for Glioblastoma. Neurologia medico-chirurgica. 2018;58(10):405–21.
6. Lomenick B, Jung G, Wohlschlegel JA, Huang J. Target identification using drug affinity responsive target stability (DARTS). Current protocols in chemical biology. 2011;3(4):163–80.
7. Pai MY, Lomenick B, Hwang H, Schiestl R, McBride W, Loo JA, Huang J: Drug affinity responsive target stability (DARTS) for small-molecule target identification. Methods in molecular biology (Clifton, NJ) 2015, 1263:287–298.
8. Cao Y, Wu J, Pan H, Wang L. Chemical Profile and Multicomponent Quantitative Analysis for the Quality Evaluation of Toad Venom from Different Origins. Molecules (Basel, Switzerland) 2019, 24(19).
9. Zhang JJ, Zhou XH, Zhou Y, Wang YG, Qian BZ, He AN, Shen Z, Hu HY, Yao Y. Bufalin suppresses the migration and invasion of prostate cancer cells through HOTAIR, the sponge of miR-520b. Acta pharmacologica Sinica. 2019;40(9):1228–36.
10. Liu F, Tong D, Li H, Liu M, Li J, Wang Z, Cheng X. Bufalin enhances antitumor effect of paclitaxel on cervical tumorigenesis via inhibiting the integrin α2/β5/FAK signaling pathway. Oncotarget. 2016;7(8):8896–907.
11. Zeino M, Brenk R, Gruber L, Zehl M, Urban E, Kopp B, Efferth T. Cytotoxicity of cardiotonic steroids in sensitive and multidrug-resistant leukemia cells and the link with Na(+)/K(+)-ATPase. J Steroid Biochem Mol Biol. 2015;150:97–111.
12. Lan YL, Zou YJ, Lou JC, Xing JS, Wang X, Zou S, Ma BB, Ding Y, Zhang B. The sodium pump α1 subunit regulates bufalin sensitivity of human glioblastoma cells through the p53 signaling pathway. 2019, 35(6):521–539.
13. Bick RJ, Poindexter BJ, Sweney RR, Dasgupta A. Effects of Chan Su, a traditional Chinese medicine, on the calcium transients of isolated cardiomyocytes: cardiotoxicity due to more than Na, K-ATPase blocking. Life sciences. 2002;72(6):699–709.
14. Menger L, Vacchelli E, Adjemian S, Martins I, Ma Y, Shen S, Yamazaki T, Sukkurwala AQ, Michaud M, Mignot G, et al. Cardiac glycosides exert anticancer effects by inducing immunogenic cell death. Science translational medicine. 2012;4(143):143ra199.
15. Sheng X, Zhu P, Qin J, Li Q. The biological role of autophagy in regulating and controlling the proliferation of liver cancer cells induced by bufalin. Oncol Rep. 2018;39(6):2931–41.
16. Liu J, Zhang Y, Sun S, Zhang G, Jiang K, Sun P, Zhang Y, Yao B, Sui R, Chen Y, et al. Bufalin Induces Apoptosis and Improves the Sensitivity of Human Glioma Stem-Like Cells to Temozolamide. Oncology research. 2019;27(4):475–86.

17. Cui X, Inagaki Y, Xu H, Wang D, Qi F, Kokudo N, Fang D, Tang W. Anti-hepatitis B virus activities of cinobufacini and its active components bufalin and cinobufagin in HepG2.2.15 cells. Biol Pharm Bull. 2010;33(10):1728–32.
18. Li Y, Yuan J, Yang Q, Cao W, Zhou X, Xie Y, Tu H, Zhang Y, Wang S. Immunoliposome co-delivery of bufalin and anti-CD40 antibody adjuvant induces synergetic therapeutic efficacy against melanoma. Int J Nanomed. 2014;9:5683–700.
19. Yuan J, Zhou X, Cao W, Bi L, Zhang Y, Yang Q, Wang S. Improved Antitumor Efficacy and Pharmacokinetics of Bufalin via PEGylated Liposomes. Nanoscale Res Lett. 2017;12(1):585.
20. Yuan J, Zeng C, Cao W, Zhou X, Pan Y, Xie Y, Zhang Y, Yang Q, Wang S. Bufalin-Loaded PEGylated Liposomes: Antitumor Efficacy, Acute Toxicity, and Tissue Distribution. Nanoscale Res Lett. 2019;14(1):223.
21. Wu Y, Pang J, Peng J, Cao F, Guo Z. Apolipoprotein E Deficiency Aggravates Neuronal Injury by Enhancing Neuroinflammation via the JNK/c-Jun Pathway in the Early Phase of Experimental Subarachnoid Hemorrhage in Mice. 2019, 2019:3832648.
22. Gurung SK, Dana S, Mandal K, Mukhopadhyay P, Mondal N. Downregulation of c-Myc and p21 expression and induction of S phase arrest by naphthalene diimide derivative in gastric adenocarcinoma cells. Chemico-Biol Interact. 2019;304:106–23.
23. Liu Q, Wang L. Prometryn induces apoptotic cell death through cell cycle arrest and oxidative DNA damage. 2019, 8(6):833–841.
24. Klaunig JE. Oxidative Stress and Cancer. Curr Pharm Design. 2018;24(40):4771–8.
25. Poprac P, Jomova K, Simunkova M, Kollar V, Rhodes CJ, Valko M. Targeting Free Radicals in Oxidative Stress-Related Human Diseases. Trends Pharmacol Sci. 2017;38(7):592–607.
26. Diaz-Vivancos P, de Simone A, Kiddle G, Foyer CH. Glutathione–linking cell proliferation to oxidative stress. Free Radic Biol Med. 2015;89:1154–64.
27. Xu Y, Liu X, Schwarz S, Hu L, Guo D, Gu Q, Schwarz W. Inhibitory efficacy of bufadienolides on Na(+),K(+)-pump activity versus cell proliferation. Biochemistry biophysics reports. 2016;6:158–64.
28. Mijatovic T, Dufrasne F, Kiss R. Na+/K+-ATPase and cancer. Pharmaceutical patent analyst. 2012;1(1):91–106.
29. Koh CH, Wu J, Chung YY, Liu Z, Zhang RR, Chong K, Korzh V, Ting S, Oh S, Shim W, et al. Identification of Na+/K+-ATPase inhibition-independent proarrhythmic ionic mechanisms of cardiac glycosides. Scientific reports. 2017;7(1):2465.
30. Schmitz F, Pierozan P, Rodrigues AF, Biasibetti H, Grings M, Zanotto B, Coelho DM, Vargas CR, Leipnitz G, Wyse ATS. Methylphenidate Decreases ATP Levels and Impairs Glutamate Uptake and Na(+),K(+)-ATPase Activity in Juvenile Rat Hippocampus. Mol Neurobiol. 2017;54(10):7796–807.
31. Lee SH, Kim MH, Park KH, Earm YE, Ho WK. K+-dependent Na+/Ca2 + exchange is a major Ca2 + clearance mechanism in axon terminals of rat neurohypophysis. The Journal of neuroscience: the official journal of the Society for Neuroscience. 2002;22(16):6891–9.

32. Li X, Fang F, Gao Y, Tang G, Xu W, Wang Y, Kong R, Tuyihong A, Wang Z: ROS Induced by KillerRed Targeting Mitochondria (mtKR) Enhances Apoptosis Caused by Radiation via Cyt c/Caspase-3 Pathway. 2019, 2019:4528616.
33. Iijima T, Mishima T, Tohyama M, Akagawa K, Iwao Y. Mitochondrial membrane potential and intracellular ATP content after transient experimental ischemia in the cultured hippocampal neuron. Neurochem Int. 2003;43(3):263–9.
34. Chen L, Lin L, Xian N, Zheng Z. Annexin A2 regulates glioma cell proliferation through the STAT3–cyclin D1 pathway. Oncol Rep. 2019;42(1):399–413.
35. Chen CY, Lin YS, Chen CH, Chen YJ. Annexin A2-mediated cancer progression and therapeutic resistance in nasopharyngeal carcinoma. Journal of biomedical science. 2018;25(1):30.
36. Mickleburgh I, Burtle B, Hollås H, Campbell G, Chrzanowska-Lightowlers Z, Vedeler A, Hesketh J. Annexin A2 binds to the localization signal in the 3' untranslated region of c-myc mRNA. FEBS J. 2005;272(2):413–21.
37. de Graauw M, Cao L, Winkel L, van Miltenburg MH, le Dévédec SE, Klop M, Yan K, Pont C, Rogkoti VM, Tijsma A, et al. Annexin A2 depletion delays EGFR endocytic trafficking via cofilin activation and enhances EGFR signaling and metastasis formation. Oncogene. 2014;33(20):2610–9.
38. Croxtall JD, Choudhury Q, Flower RJ. Glucocorticoids act within minutes to inhibit recruitment of signalling factors to activated EGF receptors through a receptor-dependent, transcription-independent mechanism. Br J Pharmacol. 2000;130(2):289–98.
39. Zhao J, Liu T, Jin S, Wang X, Qu M, Uhlén P, Tomilin N, Shupliakov O, Lendahl U, Nistér M. Human MIEF1 recruits Drp1 to mitochondrial outer membranes and promotes mitochondrial fusion rather than fission. EMBO J. 2011;30(14):2762–78.
40. Lee YG, Nam Y, Shin KJ, Yoon S, Park WS, Joung JY, Seo JK, Jang J, Lee S, Nam D, et al. Androgen-induced expression of DRP1 regulates mitochondrial metabolic reprogramming in prostate cancer. Cancer letters. 2020;471:72–87.
41. Plewes MR, Hou X, Talbott HA, Zhang P, Wood JR, Cupp AS, Davis JS. Luteinizing hormone regulates the phosphorylation and localization of the mitochondrial effector dynamin-related protein-1 (DRP1) and steroidogenesis in the bovine corpus luteum. 2020, 34(4):5299–5316.
42. Lim S, Lee SY, Seo HH, Ham O, Lee C, Park JH, Lee J, Seung M, Yun I, Han SM, et al. Regulation of mitochondrial morphology by positive feedback interaction between PKCδ and Drp1 in vascular smooth muscle cell. Journal of cellular biochemistry. 2015;116(4):648–60.
43. Montessuit S, Somasekharan SP, Terrones O, Lucken-Ardjomande S, Herzig S, Schwarzenbacher R, Manstein DJ, Bossy-Wetzel E, Basañez G, Meda P, et al. Membrane remodeling induced by the dynamin-related protein Drp1 stimulates Bax oligomerization. Cell. 2010;142(6):889–901.
44. Fonseca TB, Sánchez-Guerrero Á, Milosevic I, Raimundo N. Mitochondrial fission requires DRP1 but not dynamins. Nature. 2019;570(7761):E34–42.
45. Favaro G, Romanello V, Varanita T, Andrea Desbats M, Morbidoni V, Tezze C, Albiero M. DRP1-mediated mitochondrial shape controls calcium homeostasis and muscle mass. 2019, 10(1):2576.

46. Kalia R, Wang RY, Yusuf A, Thomas PV, Agard DA, Shaw JM, Frost A. Structural basis of mitochondrial receptor binding and constriction by DRP1. Nature. 2018;558(7710):401–5.

47. Otera H, Mihara K. Mitochondrial dynamics: functional link with apoptosis. International journal of cell biology 2012, 2012:821676.

# Figures

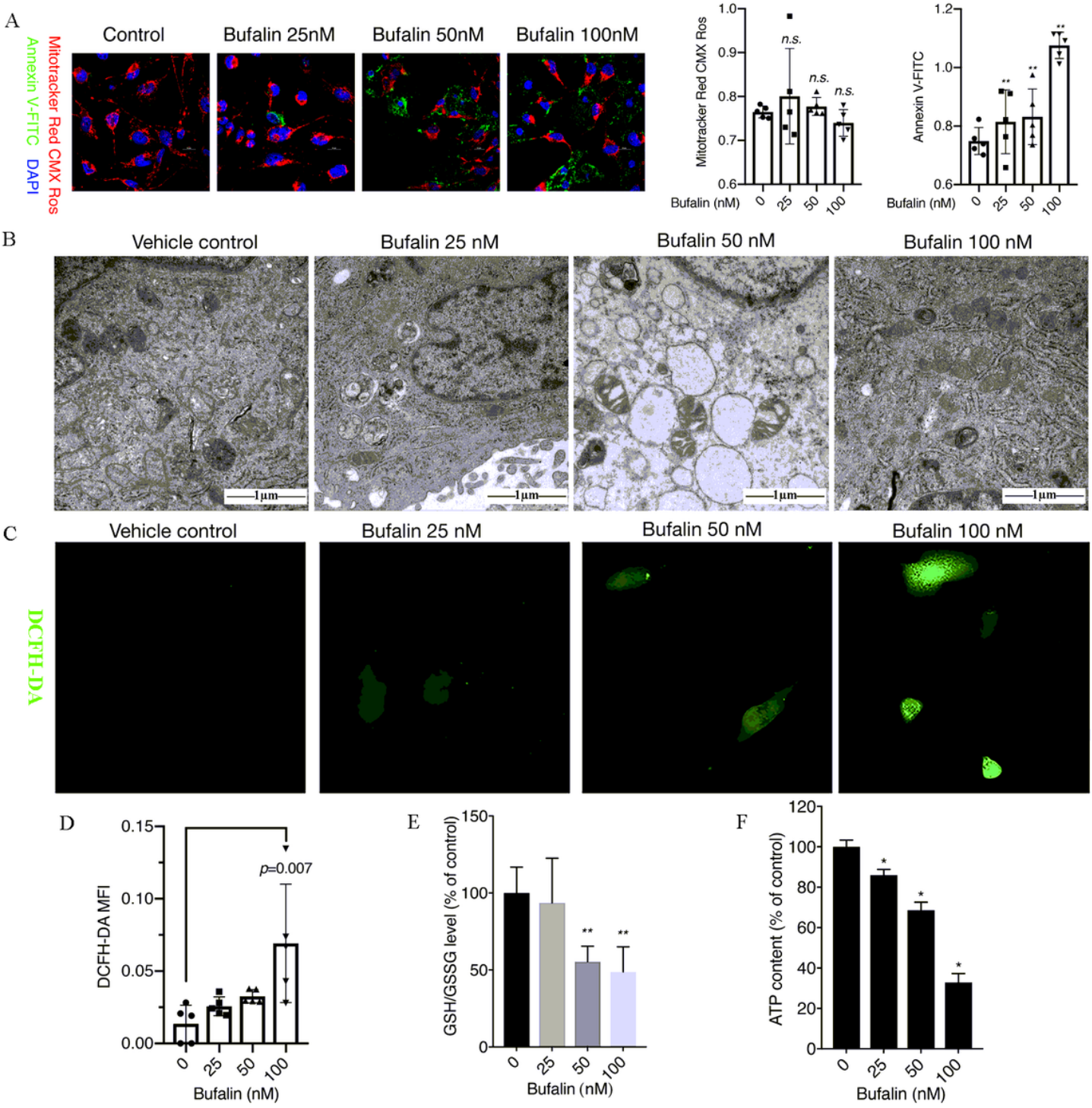


**Figure 1**

Bufalin induces cell apoptosis and oxidative stress. (A) Cell apoptosis was observed by confocal microscope after Mitotracker Red CMX Ros, Annexin V-FITC and Hoechst33342 co-staining (n=3). (B) Ultrastructure of U251 cells measured by TEM. (C) The intracellular ROS content was observed by laser confocal microscope after DCFH-DA staining (n=3). (D) The ROS level of U251 cells. (E) The ratio of GSH/GSSH in each group of cells, **p < 0.01 compared with DMSO control. (F) The intracellular ATP content of U251 cells after treated with different concentration of bufalin (n=3). *p < 0.05, **p < 0.01 compared with DMSO control.

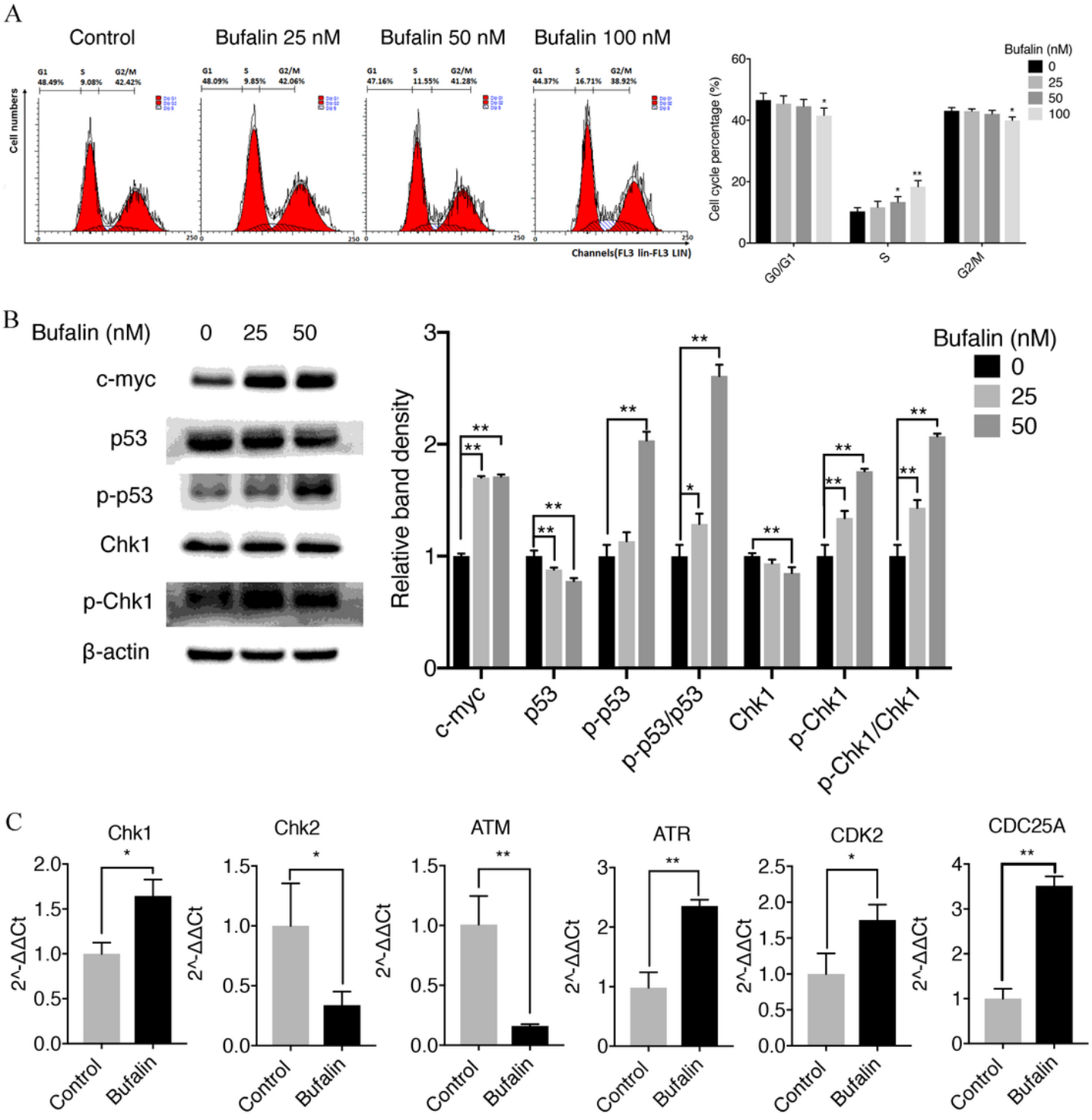

## Figure 2

Bufalin induces DNA damage and arrest the cell cycle at S phase. (A) Proportion of each phase in the cell cycle after bufalin treatment (n=3). (B) Detection of DNA damage and cell cycle related proteins by western blot (n=3). (C) Detection the mRNA levels of S-phase DNA damage related genes (n=3). *p < 0.05, **p < 0.01 compared with DMSO control.

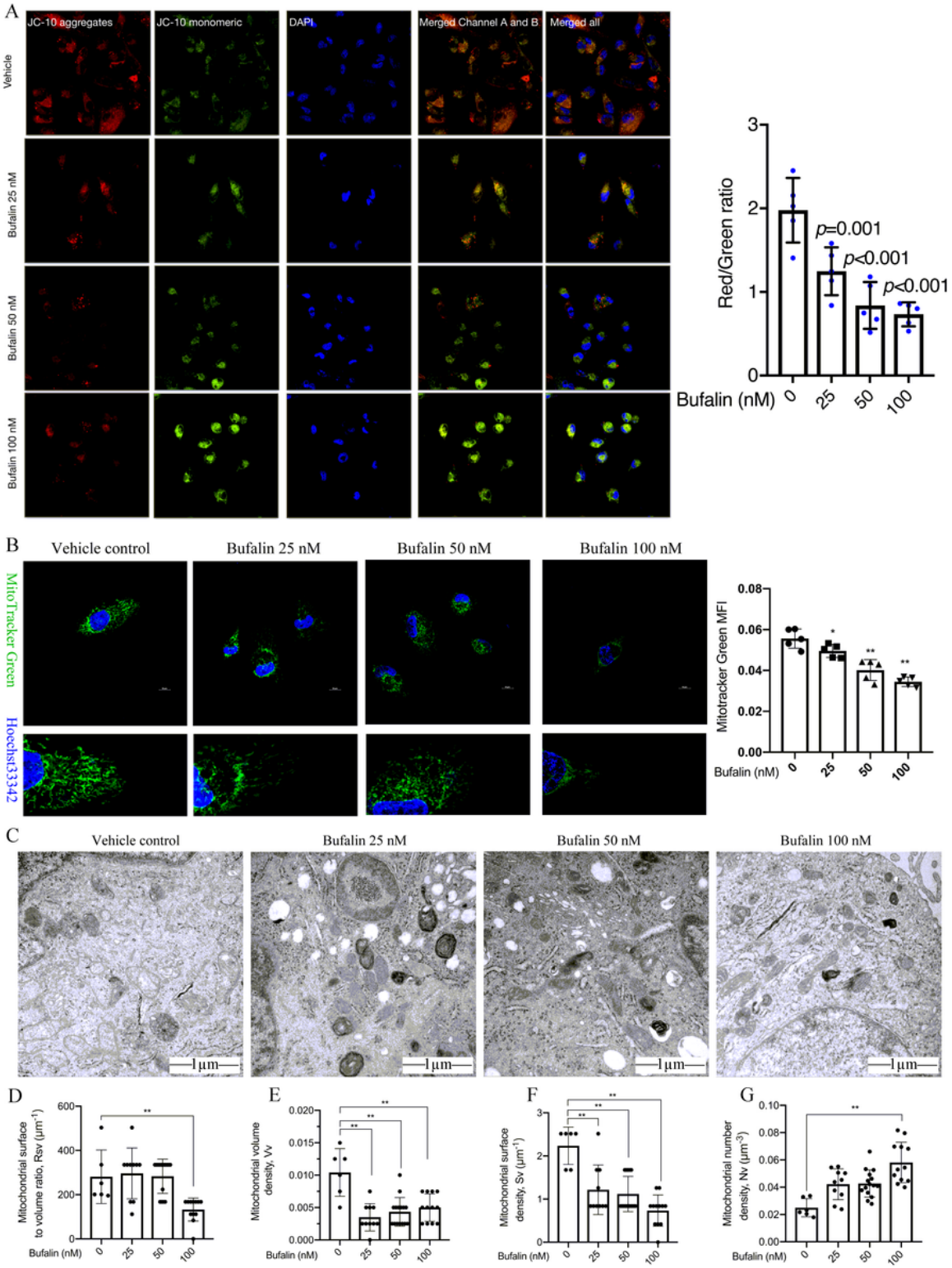


## Figure 3

Bufalin induces mitochondrial dysfunction in U251 cells. (A) Mitochondrial membrane potential of U251 cells detected by JC-10 staining (n=3). (B) Confocal microscope observation of mitochondrial morphology and distribution after Mitotracker Green and Hoechst 33342 staining (n=5). (C) Mitochondrial morphology of U251 cells observed by TEM. (D-G) Stereology theory analyzes Rsv, Vv, Sv and Nv of mitochondria. *p < 0.05, **p < 0.01 compared with DMSO control.

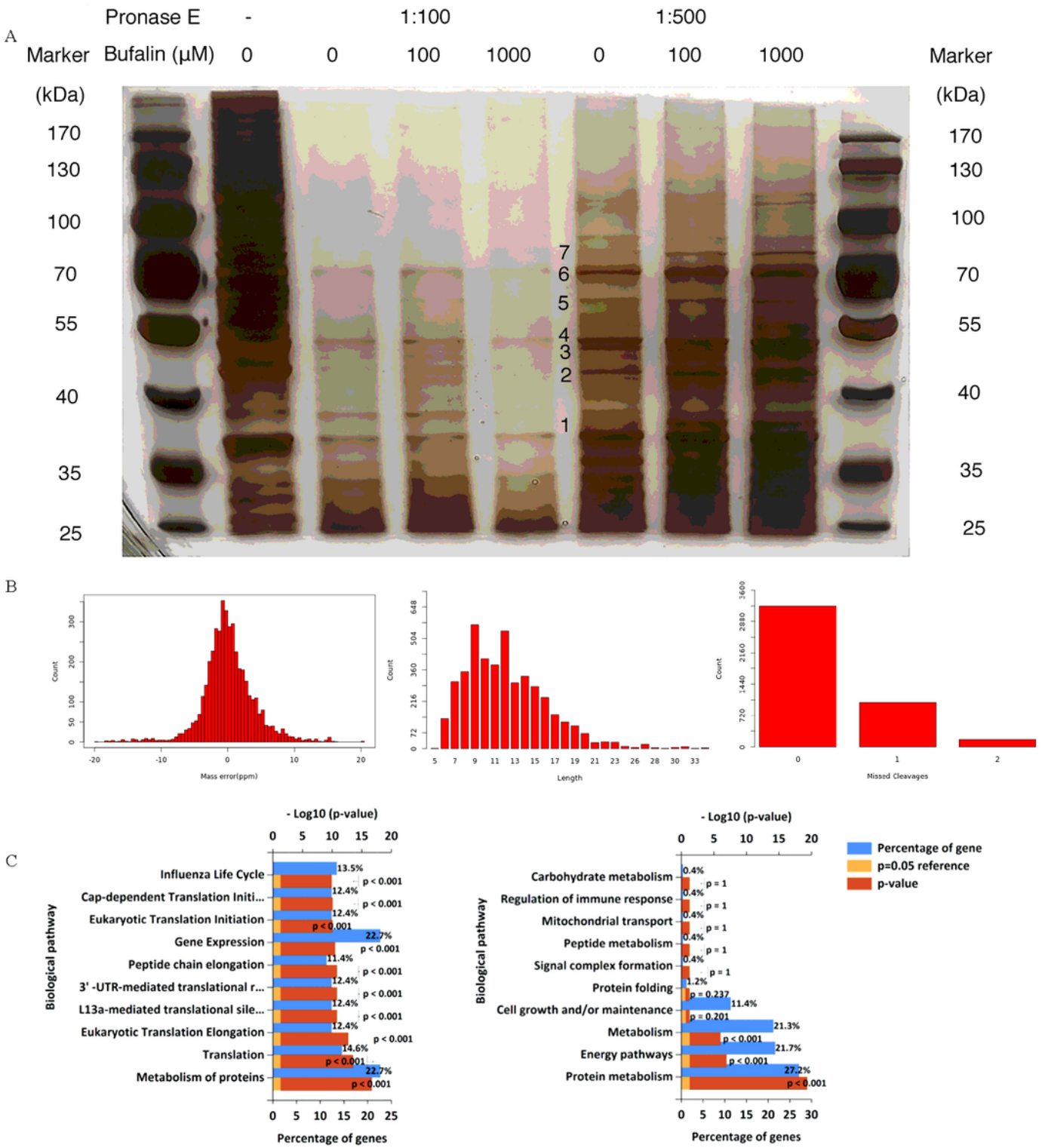


## Figure 4

Target identification of bufalin acting on U251 cells. (A) The silver staining results of DARTS-PAGE experiment. (B) The peptide length distribution, statistics of missing cleavage sites and the peptide mass deviation distribution. (C) GO function analysis of differential proteins.

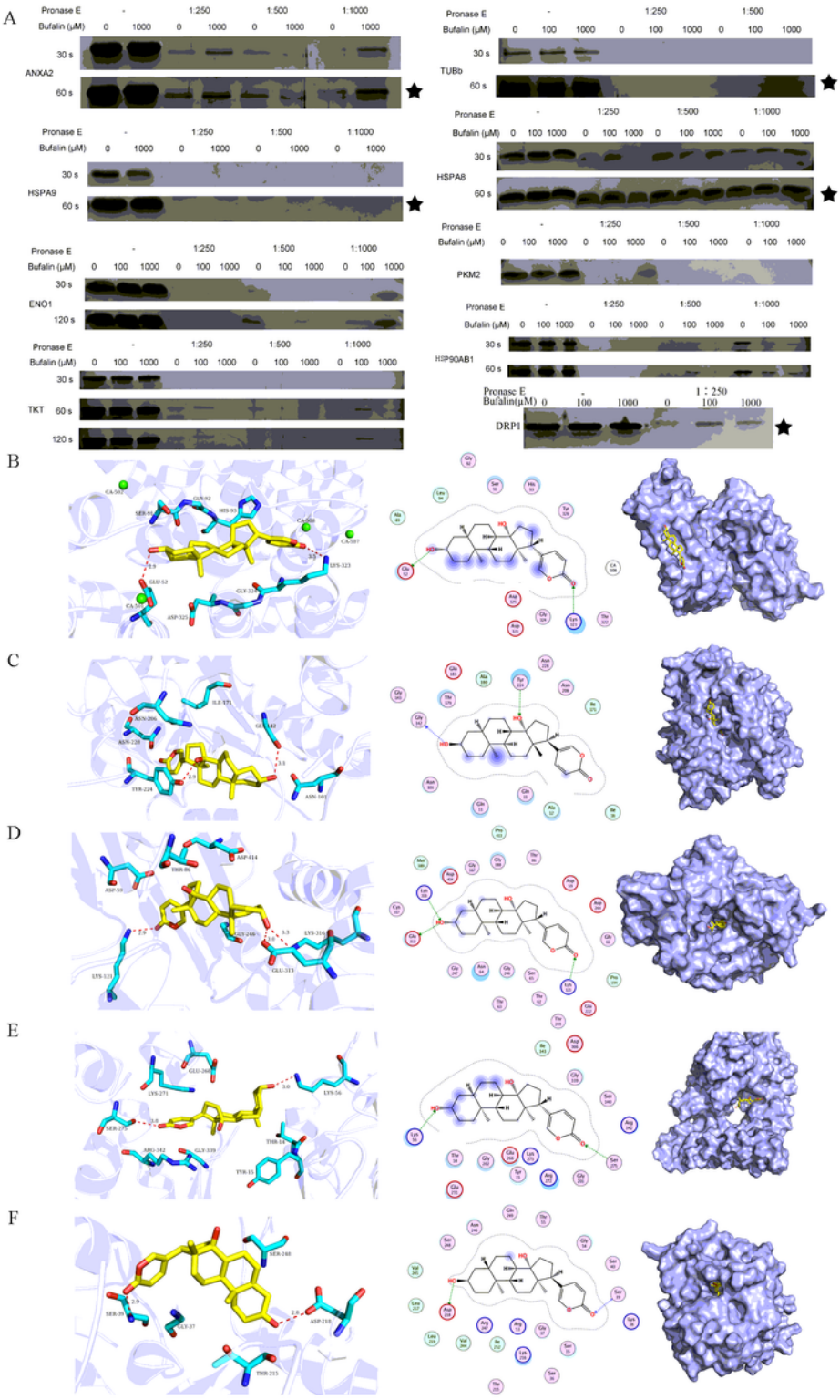


## Figure 5

The target proteins screening and verifications of bufalin. (A) Silver staining verification result of pure protein and bufalin co-incubation. (B-F) 2D, 3D and surface binding model between bufalin with Annexin

A2, TUBb, HSPA9, HSPA8, and DRP1 protein.

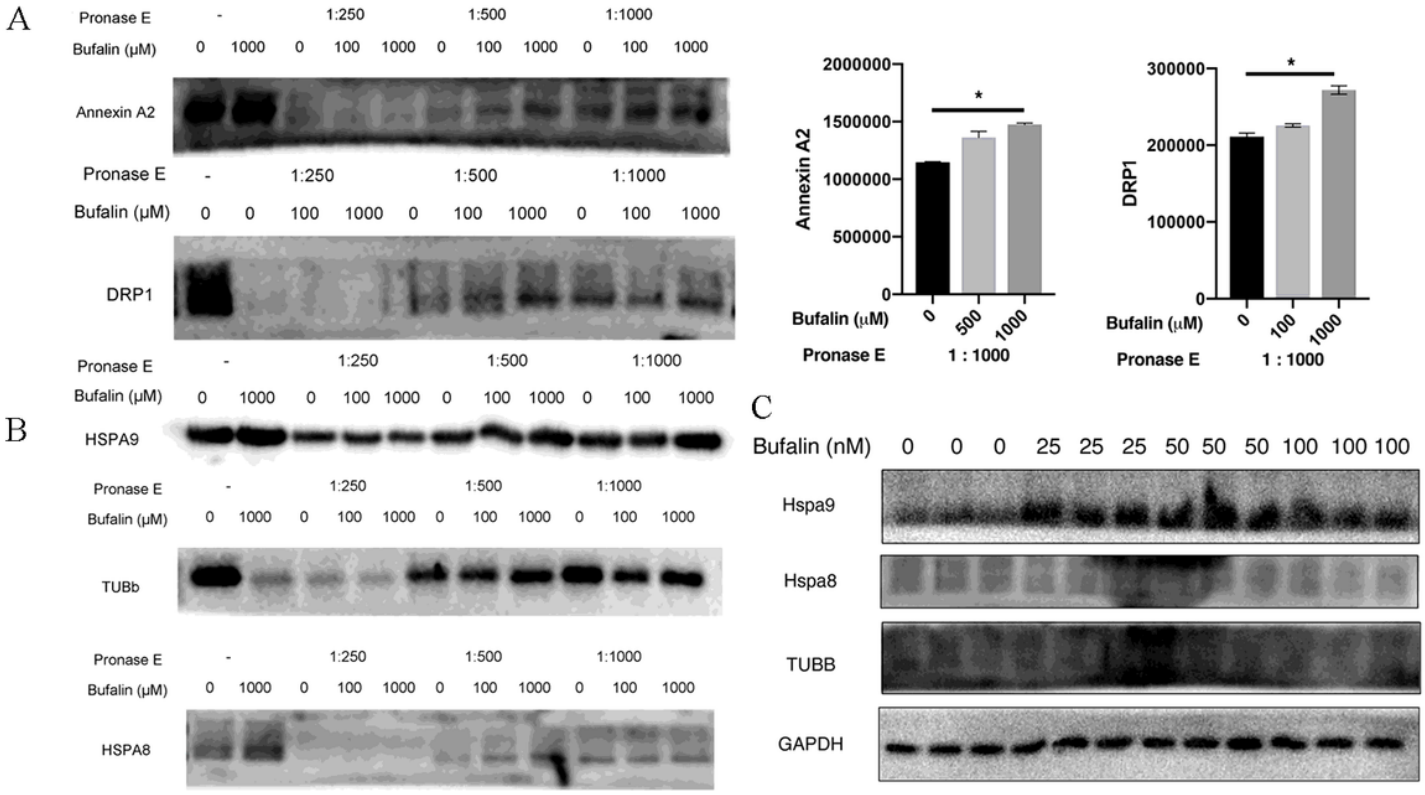


## Figure 6

The direct target of bufalin. (A) The binding ability of bufalin with Annexin A2 and DRP1 in the total protein of U251 cells verified by DARTS-Western blot, *p < 0.05, compared with DMSO control (n=3). (B) DARTS-Western blot experiment to detect the protein expression levels of HSPA8, HSPA9 and TUBb in U251 cells pure proteins after co-incubation with bufalin (n=3). (C) The protein expression levels of HSPA8, HSPA9 and TUBb in U251 cells after bufalin treatment detected by western blot (n=3).

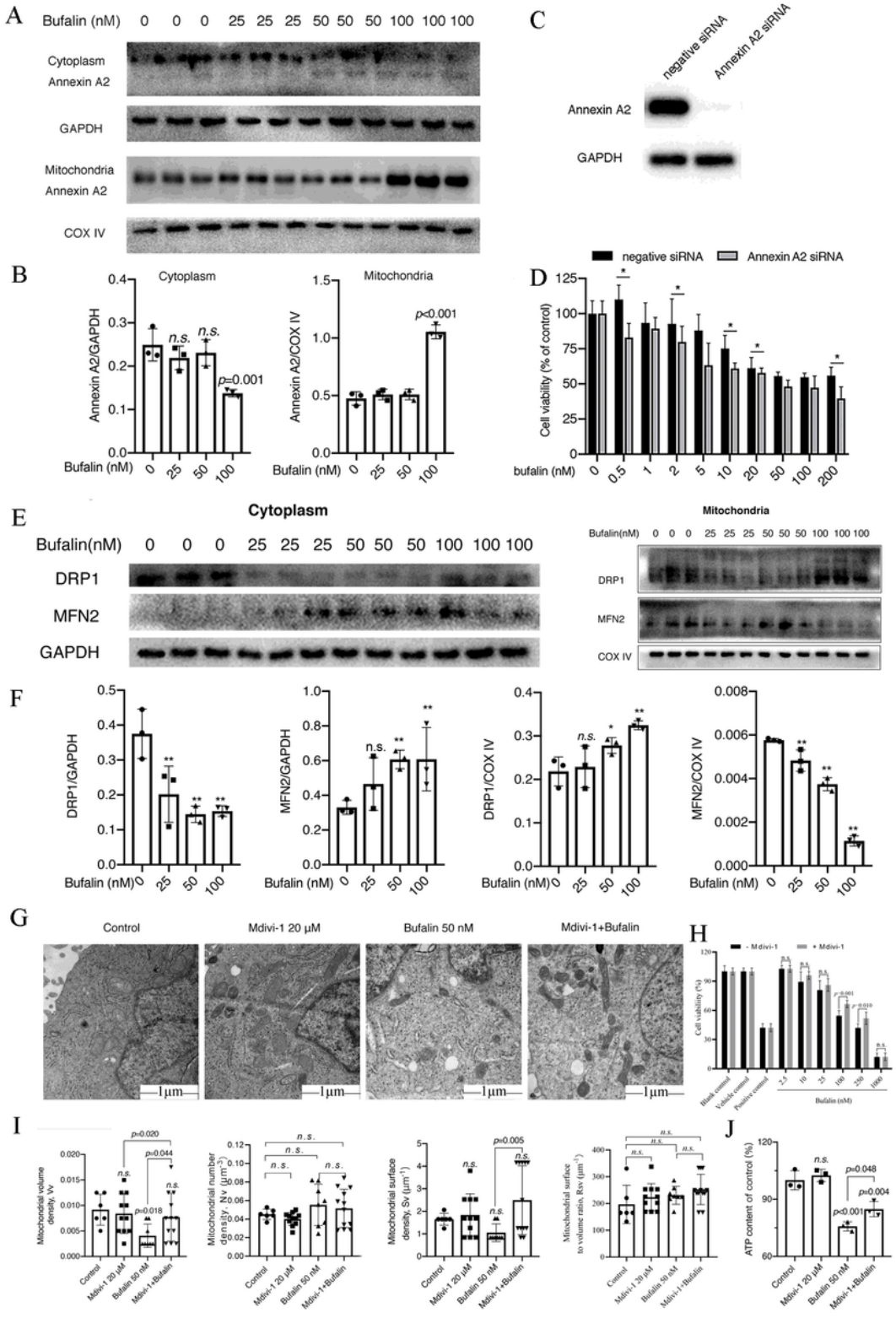


## Figure 7

Bufalin induces U251 cell apoptosis via regulating Annexin A2 and DRP1 protein. (A) The expression of Annexin A2 protein in U251 cytoplasm and mitochondrial after bufalin treatment (n=3). (B) Statistics of Annexin A2 in U251 cytoplasm and mitochondria after bufalin treatment. (C) Verification of Annexin A2 siRNA silencing effect. (D) The viability of U251 cells of Annexin A 2 silencing after bufalin treatment (n=6). (E) The expression level of DRP1 and MFN2 protein in the cytoplasm and mitochondria of U251

cells detected by western blot (n=3). (F) Statistics of DRP1 and MFN2 in U251 cytoplasm and mitochondria after bufalin treatment. (G) Mitochondrial morphology and structure of U251 cells observed by TEM (n=3). (H) Cell viability of U251 cells pretreatment with Mdivi-1 (n=6). (I) Stereology theory analyzes Rsv, Vv, Sv and Nv of mitochondria when pretreatment by Mdivi-1. (J) The intracellular ATP content of U251 cells (n=3). *p < 0.05, **p < 0.01 compared with DMSO control.

## Supplementary Files

This is a list of supplementary files associated with this preprint. Click to download.

- supplementarymaterials.doc